Drosophila pericentrin requires interaction with calmodulin for its function at centrosomes and neuronal basal bodies but not at sperm basal bodies

Brian J. Galletta[a,*], Rodrigo X. Guillen[a,*], Carey J. Fagerstrom[a], Chris W. Brownlee[b], Dorothy A. Lerit[a], Timothy L. Megraw[c], Gregory C. Rogers[b], and Nasser M. Rusan[a]

[a]Cell Biology and Physiology Center, National Heart, Lung, and Blood Institute, National Institutes of Health, Bethesda, MD 20892; [b]Department of Cellular and Molecular Medicine, University of Arizona Cancer Center, University of Arizona, Tucson, AZ 85724; [c]Department of Biomedical Sciences, Florida State University College of Medicine, Tallahassee, FL 32304

ABSTRACT **Pericentrin is a critical centrosomal protein required for organizing pericentriolar material (PCM) in mitosis. Mutations in pericentrin cause the human genetic disorder Majewski/microcephalic osteodysplastic primordial dwarfism type II, making a detailed understanding of its regulation extremely important. Germaine to pericentrin's function in organizing PCM is its ability to localize to the centrosome through the conserved C-terminal PACT domain. Here we use *Drosophila* pericentrin-like-protein (PLP) to understand how the PACT domain is regulated. We show that the interaction of PLP with calmodulin (CaM) at two highly conserved CaM-binding sites in the PACT domain controls the proper targeting of PLP to the centrosome. Disrupting the PLP-CaM interaction with single point mutations renders PLP inefficient in localizing to centrioles in cultured S2 cells and *Drosophila* neuroblasts. Although levels of PCM are unaffected, it is highly disorganized. We also demonstrate that basal body formation in the male testes and the production of functional sperm does not rely on the PLP-CaM interaction, whereas production of functional mechanosensory neurons does.**

Monitoring Editor
Monica Bettencourt-Dias
Instituto Gulbenkian de Ciência

Received: Oct 25, 2013
Revised: Jul 7, 2014
Accepted: Jul 8, 2014

INTRODUCTION

Centrosomes are cellular organelles required for microtubule (MT) organization during both interphase and mitosis (Kellogg *et al.*, 1994). They are highly complex structures made up of hundreds of proteins assembled into a core pair of centrioles and surrounding pericentriolar material (PCM). Our understanding of the role and regulation of almost all of these proteins is extremely limited. One class of centrosomal proteins that has drawn significant attention comprises those that may act to scaffold proteins within the PCM. These scaffolds, which include the proteins centrosomin (Cnn; Megraw *et al.*, 1999; Fong *et al.*, 2008; Choi *et al.*, 2010) and possibly Cep152/Asterless (Varmark *et al.*, 2007; Fu and Glover, 2012; Lawo *et al.*, 2012; Mennella *et al.*, 2012), have been suggested to recruit a series of other proteins to the centrosome. Pericentrin is believed to be the main PCM scaffolding protein that directly recruits the MT nucleation machinery—the γ-tubulin ring complex (Dictenberg *et al.*, 1998; Takahashi *et al.*, 2002; Zimmerman *et al.*, 2004). In addition, Pericentrin has been linked to ciliary function and human genetic disorders such as Majewski/microcephalic osteodysplastic primordial dwarfism type II (MOPD II) and Seckel syndrome (Jurczyk *et al.*, 2004; Anitha *et al.*, 2008; Jackson *et al.*, 2008; Rauch *et al.*, 2008; Delaval and Doxsey, 2010; Willems *et al.*, 2010; Muhlhans *et al.*, 2011). Therefore understanding all aspects of pericentrin regulation and function is critical to understanding these diseases.

This article was published online ahead of print in MBoC in Press (http://www.molbiolcell.org/cgi/doi/10.1091/mbc.E13-10-0617) on July 16, 2014.

*These authors contributed equally.

Address correspondence to: Nasser M. Rusan (Nasser@nih.gov).

Abbreviations used: CaM, calmodulin; CBD, calmodulin-binding domain; GFP, green fluorescent protein; MT, microtubule; NB, neuroblast; PACT, pericentrin-AKAP450-centrosome targeting; PCM, pericentriolar material; Pcnt, pericentrin; PLP, pericentrin-like protein.

Pericentrin's function in organizing PCM has been recognized for some time (Doxsey *et al.*, 1994; Takahashi *et al.*, 2002; Haren *et al.*, 2009; Matsuo *et al.*, 2010). Germane to this function is its ability to properly target and localize to centrosomes, potentially attaching directly to the centriole wall. This localization is mediated by a highly conserved domain called pericentrin-AKAP450-centrosome targeting (PACT) located at the C-terminus of pericentrin and its homologue, CG-NAP/AKAP450 (Gillingham and Munro, 2000). The PACT domain in isolation is sufficient for centriole targeting (Gillingham and Munro, 2000; Martinez-Campos *et al.*, 2004). In fact, the PACT domain has been used as a tool to ectopically drive the localization of other proteins to the centriole (Kishi *et al.*, 2009; Januschke *et al.*, 2013). Although sufficient for centriole localization, it is not known whether the PACT domain is necessary for pericentrin localization and function. However, two pieces of evidence are highly suggestive of its necessity: 1) Overexpression of the PACT domain in cultured cells reduces the efficiency of PCM recruitment to centrosomes, suggesting that it acts as a dominant negative to endogenous pericentrin (Gillingham and Munro, 2000). 2) All but one of the cases of primordial dwarfism mapped to pericentrin are nonsense mutations that terminate translation upstream of the PACT domain (Rauch *et al.*, 2008; Willems *et al.*, 2010). Even the one isolated case results from a single amino acid deletion, lysine 3154, in the PACT domain (Kantaputra *et al.*, 2011). Together these data point to a critical role for the PACT domain in the function of pericentrin, but a direct test of this hypothesis has not been performed.

Drosophila PLP, the orthologue to human pericentrin (Pcnt), was identified through its homology to the PACT domain (Kawaguchi and Zheng, 2004; Martinez-Campos *et al.*, 2004). PLP is also similar to Pcnt in function, as loss of PLP affects mitotic PCM architecture and cilia formation (Martinez-Campos *et al.*, 2004). Furthermore, the spatial arrangements of Pcnt and PLP in the centrosome are identical, with the PACT domain positioned near the centriole wall and the N-terminus extending away in a radial manner (Fu and Glover, 2012; Lawo *et al.*, 2012; Mennella *et al.*, 2012; Sonnen *et al.*, 2012). Given all these similarities, PLP serves as a valuable model to study pericentrins.

Pioneering work in fungi demonstrated that calmodulin (CaM) functions at the spindle pole body as a critical partner of Spc110 (*Saccharomyces cerevisiae*; Geiser *et al.*, 1993; Stirling *et al.*, 1994, 1996; Sundberg *et al.*, 1996) and PCP1 (*Schizosaccharomyces pombe*; Flory *et al.*, 2002), the functional orthologues of pericentrin. The binding sites for CaM at the C-terminus of PCP1 are highly conserved and are located within the PACT domain (Flory *et al.*, 2002). In fact, an interaction between PACT and CaM has also been shown in both humans and *Drosophila* (Flory *et al.*, 2000; Gillingham and Munro, 2000; Kawaguchi and Zheng, 2004), and biochemical analysis indicates that mutants within the CaM-binding sites can completely abrogate CaM's interaction with the C-terminus of Pcnt (Flory *et al.*, 2000; Gillingham and Munro, 2000). Furthermore, loss of the PACT-CaM interaction reduces the efficiency of PACT centrosome targeting (Gillingham and Munro, 2000). These results led to the long-standing hypothesis that this interaction is required for the proper localization and function of Pcnt and PLP. In this study, we directly test this hypothesis by investigating the importance of CaM in the function of PLP at centrosomes and basal bodies in *Drosophila*.

RESULTS

PLP requires CaM for efficient centrosome localization in vitro

Given the known interaction between the PACT domain and CAM (Gillingham and Munro, 2000), we hypothesized that CaM is essential for PLP's function at the centrosome. We began by investigating the relative localization of endogenous PLP and CaM in interphase and mitosis in *Drosophila* S2 cells. In mitosis, CaM accumulates on the entire centrosome, whereas PLP localization is more compact (Supplemental Figure S1A), consistent with CaM's known spindle pole localization (Zavortink *et al.*, 1983) and PLP's known proximity to the centriole wall (Fu and Glover, 2012; Mennella *et al.*, 2012). In interphase, PLP staining remained compact at centrioles, whereas CaM was undetectable (Supplemental Figure S1A), suggesting that PLP might not require CaM for localization in interphase. Of interest, green fluorescent protein (GFP)–CaM does localize to interphase centrioles (Supplemental Figure S1B), raising the possibility that the antibody used might not detect the centriole CaM pool due to its low levels or poor antibody access to the CaM epitope. Alternatively, GFP-CaM overexpression might force CaM onto the centriole in interphase in a nonphysiological manner.

To determine whether loss of CaM affected centrosomal PLP localization to interphase and mitotic centrioles, we reduced CaM protein levels using double-stranded RNA (dsRNA)–mediated interference in *Drosophila* S2 cells (Figure 1A and Supplemental Figure S1, C and D). Depletion of CaM revealed two very distinct phenotypes: a reduction in the average number of centrioles per cell (Figure 1B) and a reduction in PLP levels at both interphase and mitotic centrioles (Figure 1C and Supplemental Figure S1D). Identical results were obtained using Kc cells, another *Drosophila* cell line (Supplemental Figure S2, A–C). The reduction in centriole number indicates that CaM is required for centriole duplication, as previously reported (Matsumoto and Maller, 2002; Dobbelaere *et al.*, 2008). These results also indicate that CaM is necessary for the efficient localization of PLP to interphase and mitotic centrioles, as 50% of the remaining centrioles in CaM-knockdown cells show a reduction or a complete absence of PLP, a phenotype not seen in control Sas6-knockdown cells (Figure 1C and Supplemental Figure S2C). Of interest, CaM appears to be required for PLP localization to interphase centrioles, even though CaM is not detectable by antibody staining. This suggests the presence of very low levels of centriolar CaM during interphase. However, we cannot rule out the possibility that the reduced level of PLP at interphase centrosomes is the result of a defect in PLP recruitment during the previous mitosis or the consequence of an indirect effect of CaM loss, given its importance for many cellular processes.

PLP's interaction with CaM relies on the CBD2 within the PACT domain

Given the lack of information regarding the 12 putative PLP isoforms, we selected PLP^{PF} for our studies (Supplemental Figure S3A). Previously known as the "long" isoform, PLP^{PF} contains a total of 13 exons (only missing the very small exons 2, 10, and 12). We show that PLP^{PF} is a reasonable selection because it localizes to centrosomes (Supplemental Figure S3B) and fully rescues plp^{-} null animals (see later discussion). We will refer to PLP^{PF} as PLP for the remainder of the article. To identify a direct interaction between PLP and CaM, we truncated PLP into five fragments (PLP^{F1}–PLP^{F5}), taking care not to disrupt predicted coiled-coil domains (Figure 2A). These fragments were N-terminally GFP tagged and transfected into S2 cells (Supplemental Figure S4A). As expected, PLP^{F5} (containing the PACT domain) localized to centrioles (Figure 2B). Of interest, PLP^{F4} localized to centrosomes at low frequency in S2 cells (Supplemental Figure S4B) but did not show centrosomal localization in transgenic animals expressing GFP::PLP^{F4} (Supplemental Figure S4C). Taken together, these results confirm that the PACT domain is the major centrosome-targeting domain in PLP. Coimmunoprecipitation from

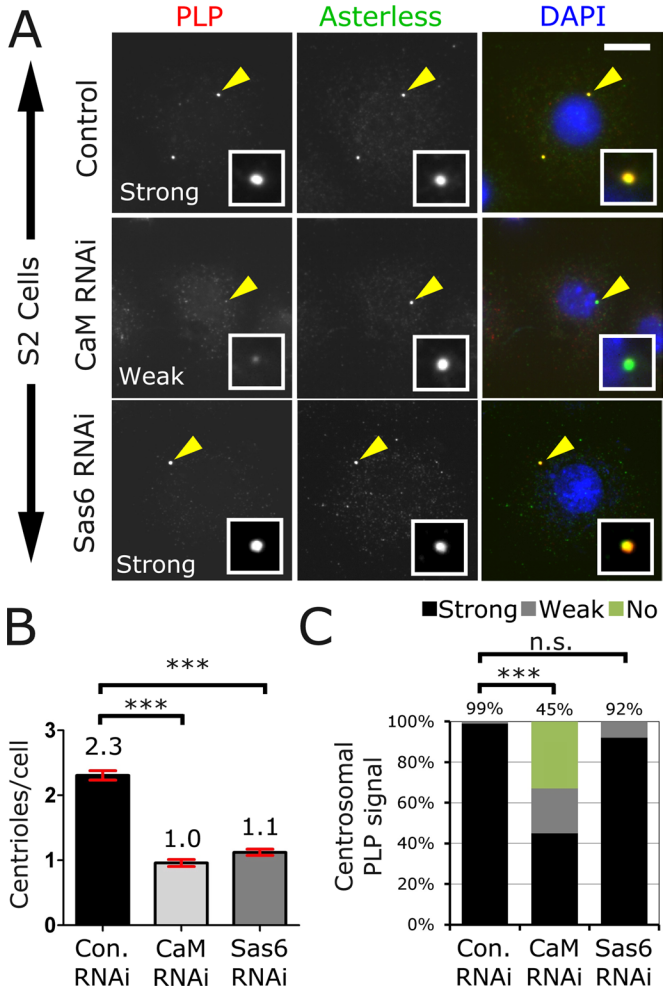

FIGURE 1: Calmodulin is required for centriole duplication and PLP targeting. (A) *Drosophila* S2 cells treated with dsRNA against control, CaM, or Sas6 were fixed and stained for PLP (red), Asterless (green), and DNA (blue). Bar, 5 μm. (B) The average number of centrioles per cell was determined for each condition. Mean is indicated on top of each bar, and SE is indicated with red brackets. Both Sas6 and CaM knockdown caused a significant reduction in the number of centrioles/cell compared with controls (analysis of variance [ANOVA] test, ***$p < 0.001$, three independent experiments, 200 cells counted per condition per experiment). (C) PLP localization strength was determined in a blind experiment and was classified as strong, weak, or no localization (three independent experiments were performed, and at least 200 cells were scored for each). The percentage of "strong" localization is shown above each column. CaM knockdown significantly reduces PLP localization to centrosomes (ANOVA followed by a paired Turkey test, ***$p < 0.001$, n.s., not significant).

transfected S2 cells shows that CaM interacts with PLP^{F5} but fails to interact with PLP^{F1}–PLP^{F4} (Supplemental Figure S4D). Yeast two-hybrid (Y2H) analysis of CaM and each of the five PLP fragments indicates that PLP^{F5} and CaM directly interact (Figure 2C).

The PACT domain contains two highly conserved CaM-binding sites, deletion of which reduces PACT targeting efficiency (Gillingham and Munro, 2000). Using a Web-based prediction program (http://calcium.uhnres.utoronto.ca/), we refined the location of the CaM-binding sites within PLP. We defined the conserved CaM Binding Domain 1 (CBD1; VESHRKALVYQKR) and CBD2 (ALAIIAIQRIKYIGR) as the regions with residues with the highest "score" of 7–9 (Yap *et al.*, 2000). These CBDs are conserved among species, with several residues absolutely conserved from flies to humans and yeast (Supplemental Figure S5). We first generated deletion mutations of CBD1 or CBD2; these deletions clearly disrupt the PLP^{F5}-CaM interaction as shown by Y2H (Figure 2D). However, it is very likely that these deletions dramatically disrupt the entire structure of the PACT domain. We therefore generated point mutations at conserved lysine (K) and arginine (R) residues in CBD1 and CBD2, which had been shown to disrupt Spc110 (yeast pericentrin) and human Pcnt interaction with CaM (Flory *et al.*, 2000; Gillingham and Munro, 2000). Mutating the Ks and Rs to alanines in CBD2 (PLP^{F5}-2KR) but not in CBD1 (PLP^{F5}-1KR) disrupted the PLP^{F5}-CaM interaction (Figure 2D). As controls, we mutated adjacent residues in each of the CBDs. The PLP^{F5}-1LV mutant did not disrupt the interaction with CaM, whereas the PLP^{F5}-2IQ reduced the interaction but did not eliminate it (Figure 2D). To determine whether these mutants can interact with CaM in cells, we first attempted coimmunoprecipitation (Co-IP) experiments by co-overexpressing CaM and each of the mutants in S2 cells. We noticed great variability in the stability of the mutant constructs, precluding a direct comparison between the mutants and control immunoprecipitations (Supplemental Figure S6A). Therefore we developed a comitochondrial-targeting (Co-MT) assay in which we express both GFP::CaM and mito-RFP-X (where X is any of the PLP^{F5} mutants; see *Materials and Methods*) from a single plasmid. In this assay, the PLP^{F5} fragments are much more stable, presumably because they are anchored to the surface of the mitochondria (Supplemental Figure S6B). We then determined whether GFP-CaM could be drawn onto the mitochondria by interacting with each of the mutant alleles. Using the Co-MT assay, we show that PLP^{F5}-2KR was unable to recruit GFP-CaM to the mitochondria, whereas PLP^{F5}-2IQ was almost indistinguishable from PLP^{F5}-WT (Supplemental Figure S6C), confirming that PLP^{F5}-2KR is unable to interact with CaM. In summary, we successfully generated a mutant that disrupts the PLP-CaM interaction (PLP^{F5}-2KR), allowing us to test the importance of this interaction.

The PLP-CaM interaction is required for targeting PLP to the centrosome

Our depletion of CaM by RNA interference (RNAi) suggests a direct role for CaM in localizing PLP to the centrosome, but possible pleiotropic effects that indirectly influence PLP localization could not be dismissed. To test whether the PLP-CaM interaction is critical, we engineered the PLP^{F5}-2KR and PLP^{F5}-2IQ mutations into full-length PLP to produce PLP^{2KR} and PLP^{2IQ}. To test the effect of these mutations on PLP, we transfected GFP fusions of each into S2 cells. We used an empirical measurement in a blind experiment to classify the strength of PLP localization to the centrosome as strong, weak, or no localization (Figure 3). There was a clear reduction in the centrosome-targeting efficiency of PLP^{2KR}, whereas the control PLP^{2IQ} was indistinguishable from PLP^{WT} (Figure 3, A and B). These data support a model in which CaM interaction at CBD2 is required for PLP targeting to the centrosome.

The PLP-CaM interaction is necessary for PLP localization and function at the centrosome in the fly

Although the PLP localization data in S2 cells suggest an important role for the PLP-CaM interaction, its physiological importance is not clear. We therefore turned to the animal model, *Drosophila*. Previous work using complete loss-of-function mutations documented three important roles for PLP in *Drosophila*: 1) a role in centrosome maturation (PCM recruitment), 2) a role in maintaining centriole integrity in meiotic cells and the proper formation of motile cilia during spermatogenesis, and 3) a role in building sensory organ cilia

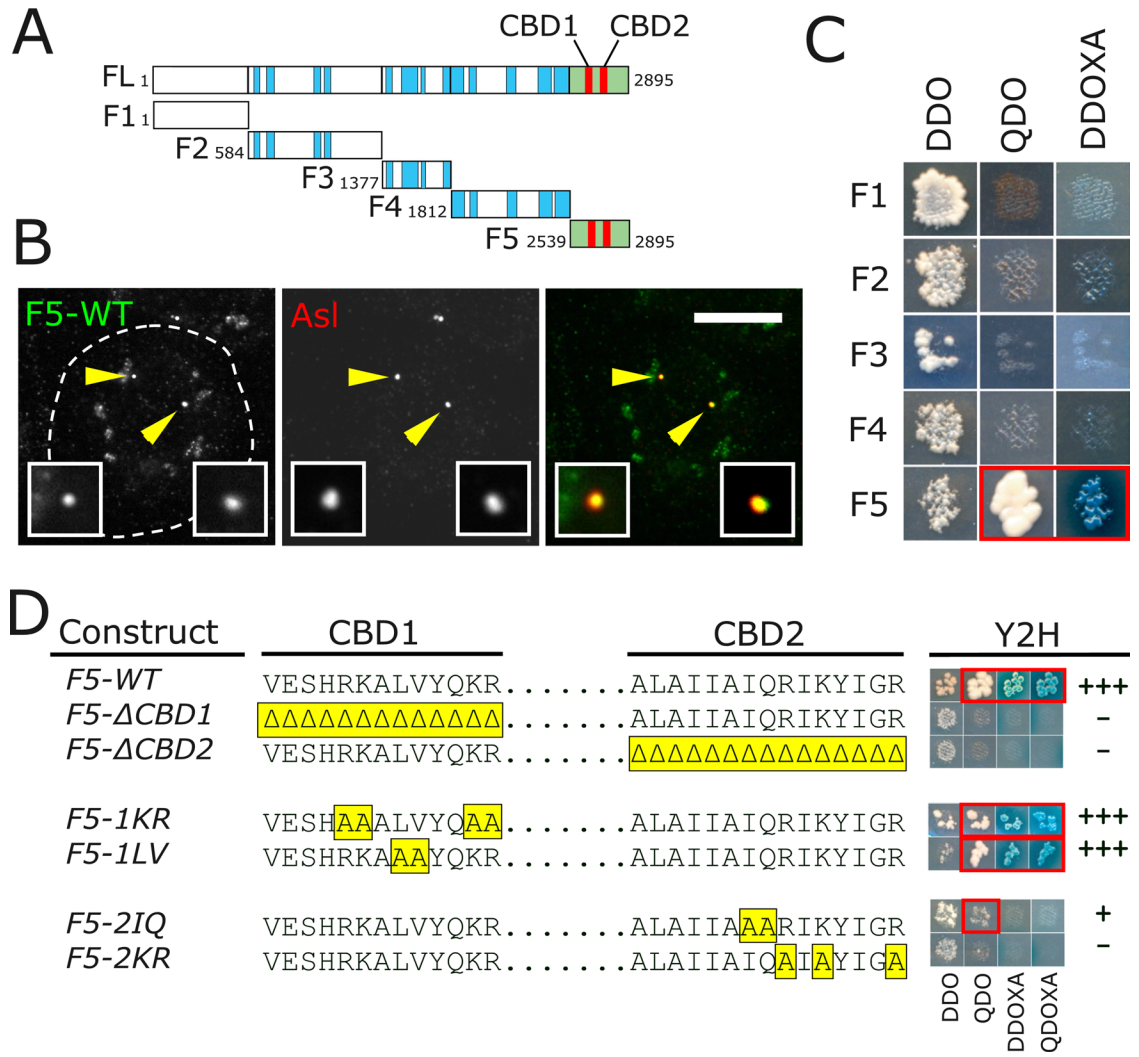

FIGURE 2: PLP binds CaM through CBD2 within the PACT domain. (A) PLP^{PF} was divided into five fragments at the indicated amino acid positions. F5 (green) includes the PACT domain, which contains CBD1 and CBD2 (red). Blue blocks indicate regions of predicted coiled-coil. (B) S2 cell transfected with F5-GFP (green) and costained for Asl (red). Insets, enlargements of the indicated centrioles (arrows). Bar, 5 μm. (C) Y2H showing direct interaction of CaM and F5 as indicated by growth on SD –Ade –His –Leu –Trp (QDO) and growth and blue color on SD –Leu –Trp +Aureobasidin A + X-α-Gal (DDOXA). (D) Amino acid sequences of CBD1 and CBD2. The yellow regions indicate the mutated residues. The Y2H column shows a picture and empirically judged strength of the interaction for each. Growth on QDO and growth and color on DDOXA and SD –Ade –His –Leu –Trp + Aureobasidin A + X-α-Gal (QDOXA) plates indicates interaction.

(Martinez-Campos *et al.*, 2004). We hypothesized that PLP requires an interaction with CaM for one or more of these functions. Our approach was to perform a detailed comparison between animals with a complete loss-of-function mutation for PLP with animals expressing mutant PLP that lacks the ability to bind CaM (PLP^{2KR}).

We began by characterizing animals expressing the *plp*^{2172} allele, a P-element insertion between exons 6 and 7 that does not produce any detectable protein, with an antibody raised against the N-terminus of PLP (Supplemental Figure S7A). We will refer to *plp*^{2172}/*Df(3L)BrdR15* as *plp*$^{-}$ throughout. To determine the effects of PLP loss of function on centrosome maturation, we analyzed the central brain neuroblasts (NBs) from control and *plp*$^{-}$ mutant flies for the ability of centrosomes to recruit the PCM component Cnn during mitosis (Figure 4A). Given the known differences between apical and basal PCM amounts and behavior in these cells (Rebollo *et al.*, 2007; Rusan and Peifer, 2007), we measured the levels of Cnn at each centrosome independently. *plp*$^{-}$ NBs showed a significant reduction in Cnn at both the apical and basal centrosomes in metaphase (Figure 4A and Supplemental Figure S8, genotype C vs. genotype 1). We also noticed a general disorganization of the PCM throughout mitosis (Figure 4A), similar to what was described previously (Martinez-Campos *et al.*, 2004). This disorganization seems to be more prominent in NBs, as we were unable to detect disorganization of PCM in mitotic (metaphase) spermatogonia (Supplemental Figure S7B). To quantify the disorganization in NB, we measured centrosome circularity (see *Materials and Methods*). In control NBs, centrosomes are fairly circular (0.9, where 1 is perfectly circular), whereas in *plp*$^{-}$ NBs, centrosomes are much more disorganized, showing significantly reduced circularity (0.7; Figure 4C, C vs. Figure 1). In the mutant there is frequently additional PCM outside of the measured region. As such, this circularity measurement is likely an underestimate of the disorganization because it measures only PCM

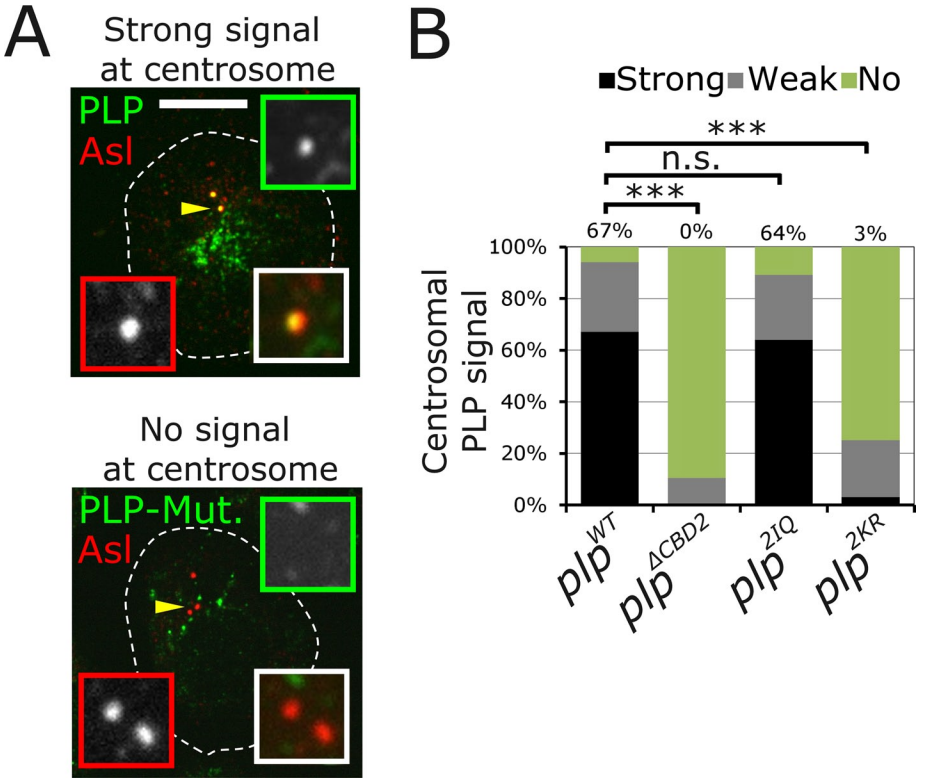

FIGURE 3: PLP centrosome targeting is disrupted by mutating CBD2. (A) Representative images of S2 cells transfected with GFP-PLP^{PF} or each of the CBD2 mutants (green). Cells were stained for Asl (red) to identify centrioles. The localization strength of GFP on the centriole was determined empirically to be strong (top), no signal (bottom), or weak (anything between these two levels). Bar, 5 µm. (B) PLP localization strength at the centrosomes was determined for indicated genotypes. At least three independent experiments were performed, and >150 cells were scored. The percentage of "strong" localization is indicated above each column. PLP localization was significantly reduced in PLP$^{\Delta CBD2}$ and PLP^{2KR} (ANOVA followed by a paired Turkey test, ***$p < 0.001$) but was normal in PLP^{2IQ} (n.s., not significant).

that is contiguous with the centrosome. This disorganization was seen in both apical and basal centrosomes equally and is also seen in *plp*^{5} (Supplemental Figure S7C), a hypomorphic allele (Martinez-Campos *et al.*, 2004) resulting from a nonsense mutation we mapped to residue Q1900 (Supplemental Figure S3A). Of interest, despite the disorganization of the centrosomes, previous reports indicate that the centrosomes in *plp*$^{-}$ neuroblasts can assemble functional spindles (Martinez-Campos *et al.*, 2004; Lerit and Rusan, 2013). Together these data confirm that PLP is required for proper PCM levels and organization during mitosis.

To test our hypothesis that PLP requires its interaction with CaM for localization and function in vivo, we generated transgenic animals expressing each of three GFP-tagged transgenes driven by the ubiquitin promoter: 1) wild-type PLP::GFP (referred to as *plp*^{WT}), 2) PLP-2IQ::GFP (referred to as *plp*^{2IQ}), and 3) PLP-2KR::GFP (referred to as *plp*^{2KR}). We selected transgenic animals that produce similar amounts of protein, as analyzed by Western blotting (Supplemental Figure S9A) and by measuring the cytoplasmic levels of GFP fluorescence (Supplemental Figure S9B). We next introduced each of these transgenes into the *plp*$^{-}$ background to produce the following genotypes: 1) *plp*^{WT}; *plp*$^{-}$ (rescue fly), 2) *plp*^{2IQ}; *plp*$^{-}$ (control mutant), and 3) *plp*^{2KR}; *plp*$^{-}$ (CaM interaction mutant). Inexplicably, on a Western blot, all three transgenes in the mutant background show a detectable band at the endogenous PLP size (Supplemental Figure S9A, blue asterisks). However, detailed PCR genotyping confirms that the endogenous PLP locus is disrupted in all three genotypes (Supplemental Figure S9C). It may be that this lower band represents a truncation of the GFP-tagged protein or that *plp*^{2172} produces a protein product, normally undetectable, that is somehow stabilized in the presence of a transgene. Most important for this study, whatever its origin, this product is nonfunctional, as it is unable to rescue the *plp*$^{-}$ mutant phenotype (see later discussion).

To determine the effect of disrupting the PLP-CaM interaction on PLP localization and centrosome function in NBs, we analyzed brains from *plp*^{WT}; *plp*$^{-}$, *plp*^{2IQ}; *plp*$^{-}$, and *plp*^{2KR}; *plp*$^{-}$ flies (Figure 4B). Analysis of apical and basal mitotic centrosomes revealed a significant (~70%) decrease in *plp*^{2KR} levels as compared with *plp*^{WT} (Figure 4D, genotype 2 vs. genotype 3). Despite this decrease in *plp*^{2KR} at the centrosome, analysis of PCM shows no reduction in Cnn levels on either the apical or basal centrosomes (Supplemental Figure S8B, genotype 5 vs. genotype 6). However, centrosome circularity (shape) was significantly altered in *plp*^{2KR}; *plp*$^{-}$ NBs as compared with *plp*^{WT}; *plp*$^{-}$ (Figure 4C, genotype 2 vs. genotype 3) and *plp*^{2IQ}; *plp*$^{-}$ (Figure 4C, genotype 2 vs. genotype 4). Of note, the expression of the *plp*^{2KR} transgene in a wild-type background shows a slight dominant effect that increases PCM levels (Supplemental Figure S8, genotype 2 vs. genotype 3) but has no dominant effect on centrosome circularity (Supplemental Figure S9D, genotype 2 vs. genotype 3). Taken together, our data in the animal strongly indicate that the PLP-CaM interaction is required to target/anchor PLP to the centrosome and organize PCM but is not required to recruit the proper amount of PCM.

The PLP-CaM interaction is critical for mechanosensation but dispensable for motile sperm formation

A second phenotype previously described in *plp*$^{-}$ animals is the "uncoordinated" phenotype, resulting from the failed formation of mechanosensory cilia (Martinez-Campos *et al.*, 2004). These *plp*$^{-}$ flies often fail to eclose properly, but if they manage to do so, they lie incapacitated. To determine whether the PLP-CaM interaction is required for mechanosensation, we assayed adult flies from the following genotypes for coordination: *plp*^{WT}; *plp*$^{-}$, *plp*^{2KR}; *plp*$^{-}$, and *plp*^{2IQ}; *plp*$^{-}$. Of importance, both *plp*^{WT} and *plp*^{2IQ} completely rescue fly viability, allowing us to generate stable stocks of *plp*^{WT}; *plp*$^{-}$ and *plp*^{2IQ}; *plp*$^{-}$ (Figure 5A). In contrast, *plp*^{2KR}; *plp*$^{-}$ flies display severe uncoordination, indistinguishable from the *plp*$^{-}$ mutant flies. To investigate the cause of this phenotype further, we imaged the basal bodies (marked by the centriole protein Ana1::tdTomato; Blachon *et al.*, 2009) of the chordotonal neurons in the *Drosophila* Johnston's organ (Figure 5, B and C). Each chordotonal neuron contained two centrioles as marked by Ana1::tdtomato, but PLP^{WT} protein was enriched on the centriole adjacent to the scolopale rod. This localization suggests that PLP is localized to the basal body and

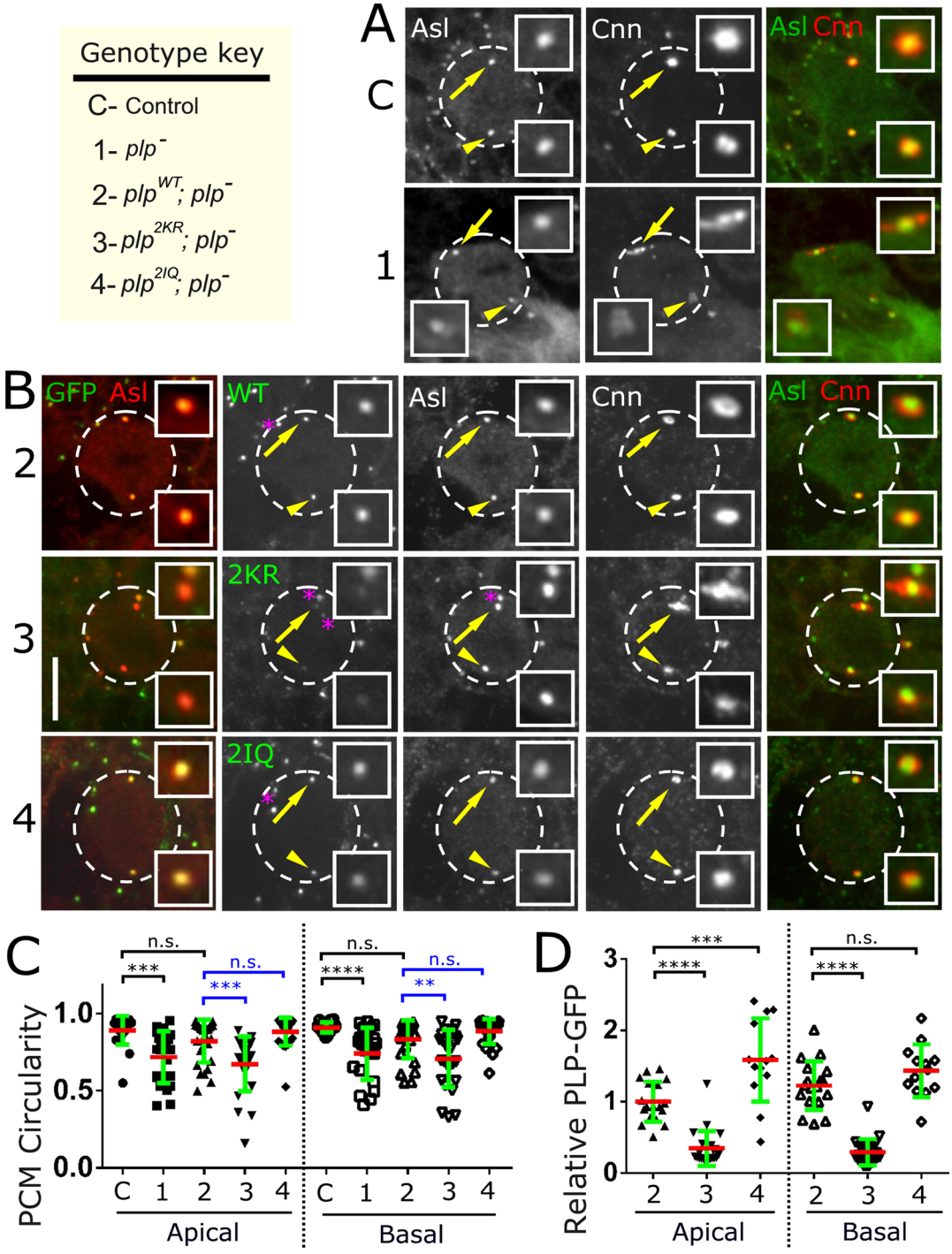

FIGURE 4: The PLP-CaM interaction is required for proper PCM organization in neuroblasts. (A) Metaphase NBs from control (genotype C) and *plp*⁻ (genotype 1) flies were stained for Asl (green) to detect centrioles and Cnn (red) to detect PCM. Enlargements of the apical (arrow) and basal (arrowhead) centrosomes. (B) NBs from animals expressing the indicated transgenes (GFP, green) in the mutant *plp*⁻ background. NBs were strained for Asl (red, left) to detect centriole and Cnn (red, right) to detect PCM. All numbers refer to the genotype key (top left corner). Images are maximum intensity projections of the entire NB volume. Bar, 10 µm. (C, D) Circularity and GFP measurements were performed on at least 15 apical and 15 basal centrosomes for the indicated genotypes. Two independent ANOVA tests (blue and green bars above the graph) followed by a paired Turkey test were performed for each of the apical and basal centrosomes. (C) Circularity measurements show a significant centrosome shape change in *plp*⁻ (genotype 1, ***$p < 0.001$, ****$p < 0.0001$) when compared with control (genotype C), but this was rescued by plp^{WT} (genotype 2, n.s., not significant). Circularity was disrupted in the plp^{2KR} mutant (genotype 3, ***$p < 0.001$, **$p < 0.01$) but not the plp^{2IQ} mutant (genotype 4, n.s., not significant). (D) Centrosomal GFP signal was normalized to apical plp^{WT} levels (genotype 2). plp^{2KR} levels are significantly reduced on the apical and basal centrosomes (genotype 3, ****$p < 0.0001$). plp^{2IQ} levels were higher than those of plp^{WT} on the apical centrosome (genotype 4, ***$p < 0.001$), which could be attributed to the slightly higher expression of the plp^{2IQ} transgene. No significant difference was measured on the basal plp^{2IQ} centrosome.

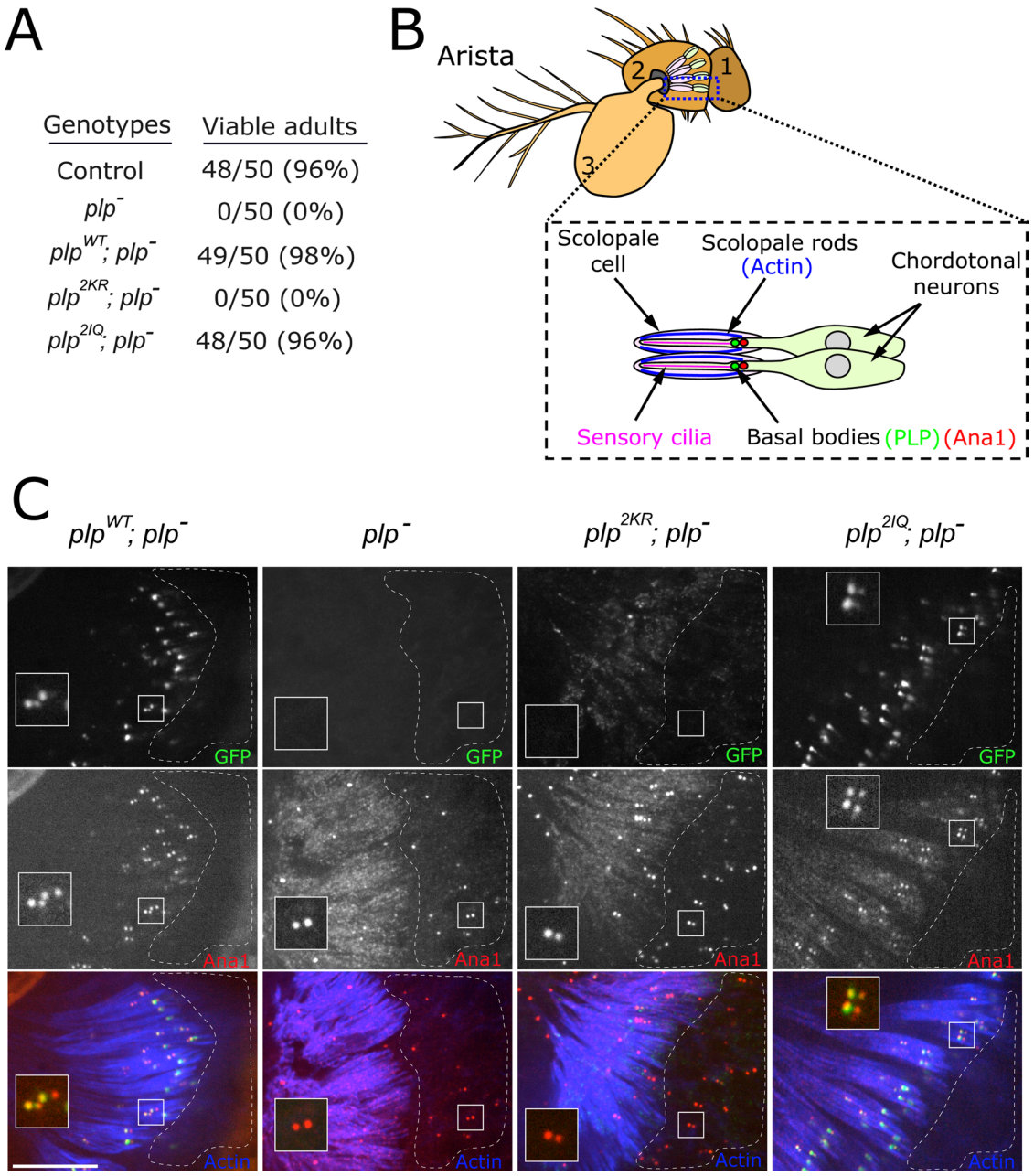

FIGURE 5: PLP requires interaction with CaM to localize to neuronal basal bodies. (A) Flies of the indicated genotype were determined to be viable if they fully eclosed and were motile in the vial. One hundred percent of the *plp*⁻ and *plp*^{2KR} individuals were incapacitated and scored "not viable." (B) Diagram indicating the location of the chordotonal neurons in the second antennal segment. (C) Actin (blue), PLP::GFP expressed from the indicated transgenes (green), and Ana1::tdTomato in chordotonal neurons. Inset, basal bodies of chordotonal neurons. Unlike *plp*^{WT} and *plp*^{2IQ}, the *plp*^{2KR} allele was incapable of localizing to basal bodies, although centrioles still formed and were randomly positioned in the area of the neural cell bodies (dashed region). Bar, 10 μm.

not the daughter centriole, consistent with a role for PLP in basal body function. As expected, PLP does not appear to be required for centriole formation/duplication (Lerit and Rusan, 2013), as centrioles were found in the *plp*^{2KR} chordotonal neurons. However, unlike the controls (*plp*^{WT} and *plp*^{2IQ}), *plp*^{2KR} centrioles were located within the cell bodies and not near the scolopale rods (dashed region, Figure 5C), similar to the complete loss-of-function *plp*⁻ mutant. Of importance, centrioles in *plp*^{2KR} neurons did not recruit PLP^{2KR} protein. These data indicate that the PLP-CaM interaction is critical for PLP function in neuronal basal bodies. Further work will be required to determine whether PLP serves a role in the centriole-to-basal body transition or its role is to assist in proper basal body membrane docking and positioning. Either way, these data offer an explanation for the absence of cilia in *plp*⁻ mutants (Martinez-Campos *et al.*, 2004).

The third and final characterized role for PLP is in the proper formation of motile sperm (Martinez-Campos *et al.*, 2004). Commonly, mutations in centrosome proteins that have an effect on mechanosensation also display defects in male fertility due to defective basal body formation (Martinez-Campos *et al.*, 2004; Basto *et al.*, 2006; Blachon *et al.*, 2008). Given that *plp*^{2KR} was unable to

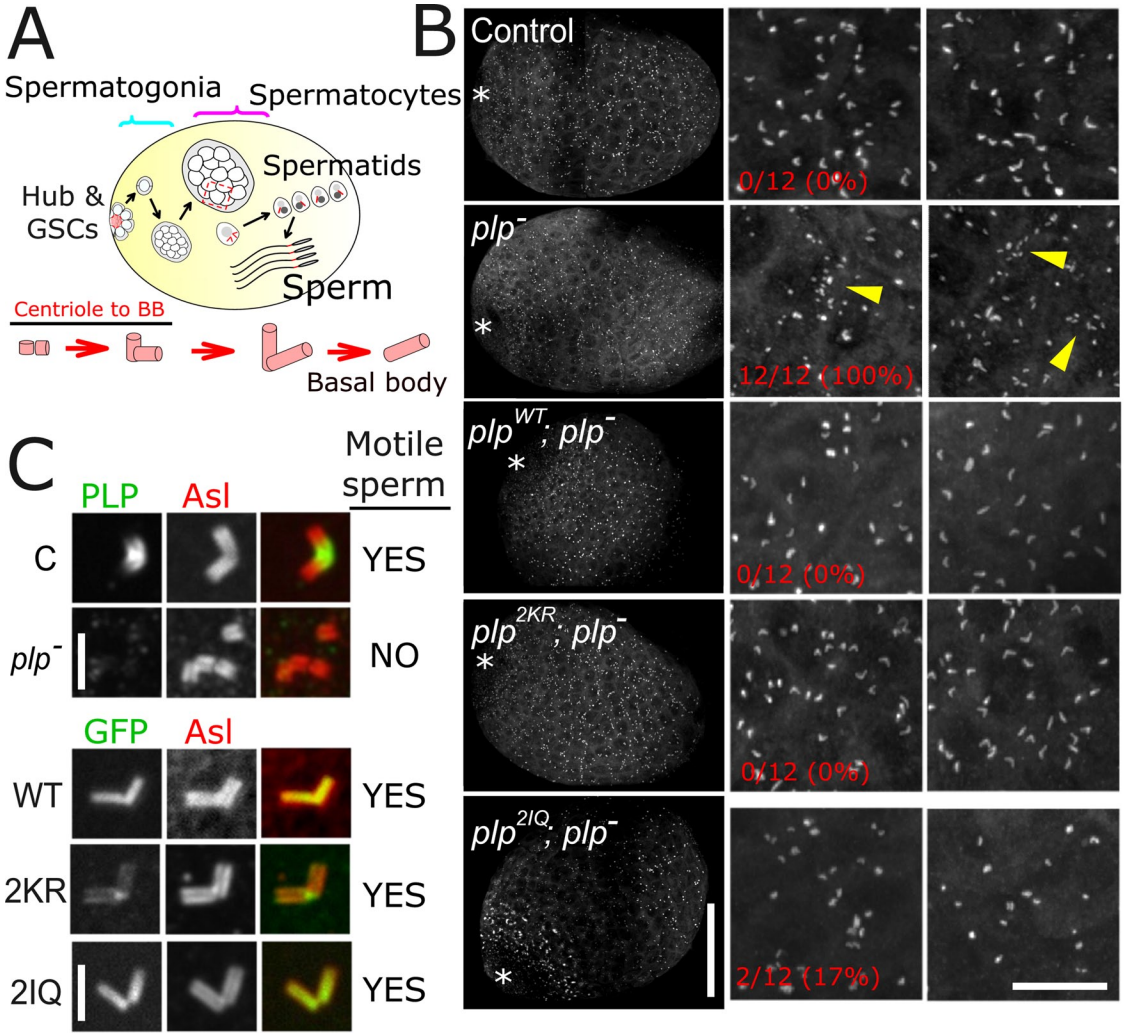

FIGURE 6: PLP does not require interaction with CaM for its role in spermatogenesis. (A) Cartoon representation of the centriole-to–basal body (BB) transition during spermatogenesis. (B) Testes from third-instar larvae of the indicated genotypes (12 testes from six larvae each). Testes were visually scored to contain abnormal centriole fragments, as clearly seen in the *plp*⁻ testes. The number of testes in which abnormal centriole fragments were observed over the total number scored is indicated on the left for each genotype. All the transgenes, including plp^{2KR}, fully rescued the *plp*⁻ centriole fragmentation. Asterisks indicate the location of the stem cell niche, termed the hub. At this stage, the gross morphology of testes of all genotypes appeared normal. The two right columns are random enlargements from the low-magnification image, intended to highlight the fragmentation phenotype. Bars, 50 μm (left), 15 μm (right enlargement). (C) Enlargements of a single centriole pair from spermatocytes of each of the indicated genotypes. Control and *plp*⁻ testes were stained for endogenous PLP (green), and the transgenes were imaged using the GFP signal. Sperm motility was determined by eye through a stereomicroscope after disruption of seminal vesicles. Bar, 2 μm.

localize to neuronal basal bodies or rescue uncoordination, we expected plp^{2KR}; *plp*⁻ animals to produce immotile sperm, similar to the *plp*⁻ mutants. We dissected male testes and analyzed the centriole-to-basal body transition (Figure 6A and Supplemental Figure S10). We found that the *plp*⁻ mutants display the previously reported giant centriole fragmentation phenotype (n = 12/12, 100%), although normal basal bodies can also be found in abundance (Figure 6, B and C). Unexpectedly, plp^{2KR} completely rescues the centriole fragmentation phenotype, with centrioles reaching normal lengths in mitosis and meiosis (Figure 6, B and C, n = 0/12, 0% fragmented centrioles). Furthermore, sperm dissected from plp^{2KR}; *plp*⁻ seminal vesicles were motile, similar to plp^{WT}; *plp*⁻ controls. Unfortunately, fertility could not be tested because these uncoordinated flies are unable to mate. Unlike sensory neuron basal bodies, we found that the plp^{2KR} was able to localize to sperm basal bodies, albeit at low levels (Figure 6C). Together these data suggest that giant centriole formation and the production of functional sperm can proceed with very little PLP localized to the centriole and do not rely on the PLP-CaM interaction.

DISCUSSION

Pericentrin has been recognized for many years for its role in scaffolding centrosomal proteins (Doxsey, 1994). A key aspect of this role is likely its physical orientation within the centrosome, where the PACT domain is anchored near the centriole wall and the N-terminus extends outward (Fu and Glover, 2012; Lawo *et al.*, 2012; Mennella *et al.*, 2012). Understanding how the PACT domain is tethered and regulated is important for understanding the function of

Genotype	CaM Interaction?	Viable adults?	Centrosome targetting?	Circular centrosomes?	Normal PCM levels?	Motile sperm?	Coordinated files?
Control	Yes	Yes	Yes	Yes	Yes	Yes	Yes
plp^{-}	–	No	–	No	No	No	No
plp^{WT}; plp^{-}	Yes	Yes	Yes	Yes	Yes	Yes	Yes
plp^{2KR}; plp^{-}	No	No	~30%	No	Yes	Yes	No

These results show that PLP's function in organizing PCM and producing functional mechanosensory cilia rely on its interaction with CaM, whereas its function to recruit normal levels of PCM and generate motile cilia does not.

TABLE 1: Summary of the findings of this study.

pericentrin. One possible method of regulating the PACT domain is through its highly conserved CaM-binding domains (CBD1 and CBD2). Our work investigates the role of CaM binding in the context of full-length pericentrin. More important, we demonstrate the importance of this interaction in an animal model system by genetically removing endogenous PLP and providing PLP carrying specific mutants from transgenes expressing normal amounts of protein.

We began by investigating the effect of the loss of CaM on PLP centrosome localization. Although complicated by possible indirect effects, CaM knockdown reduces the level of PLP at centrioles in cultured cells. We attempted similar experiments in the animal but were unsuccessful in analyzing tissue from zygotic homozygous-null CaM mutation (CaM^{n339}) or RNAi knockdown (see *Materials and Methods*) because they die as early larvae. We also attempted to generate clones of CaM-null cells using the hs-FLP system (see *Materials and Methods*) but were unable to recover any cam^{-} clones, suggesting that cells lacking CaM do not survive. We concluded from these harsh experiments that our hypothesis must be addressed using a more precise method of perturbing the PLP-CaM interaction.

The CBDs in the PACT domain show high evolutionary conservation, suggesting not only similar CaM-binding properties among species, but also similar regulation and function. Deletion of either CBD1 or CBD2 disrupts the PACT-CaM interaction, suggesting a cooperative binding model. This is consistent with the analysis of the Pcnt PACT domain (Gillingham and Munro, 2000). However, the point mutations generated here revealed a stronger dependence on CBD2, suggesting that CBD1 is insufficient for CaM binding but might serve to modulate the CaM-CBD2 interaction. For the purposes of this study, we sought to generate a PLP allele that completely lacks the ability to bind CaM, and we were successful with the plp^{2KR} allele. We note that although this mutant disrupts the interaction of PLP with CaM, it remains a formal possibility, as is the case with any mutation in any protein, that the amino acid changes we generated in the PACT domain might disrupt the interaction of PLP with a hitherto-unidentified binding partner. Our overexpression analysis in cultured cells and our replacement of endogenous PLP with mutant transgenes in animals reveal that the conserved CBDs in the PACT domain serve a critical role in PLP targeting and centrosome function in vivo. Although this mutant reduced the amount of PLP localized to the centrosome by 70%, some PLP was still able to localize to the centrosome. This indicates that there must be an additional, although less robust, mechanism for recruiting PLP to the centrosome that does not require the PLP-CaM interaction.

Our results uncovered roles for PLP that depend on its CaM interaction and others that do not (Table 1). Therefore the plp^{2KR} mutant is a true separation-of-function allele that begins to tease apart the complex function of PLP. As it relates to centrosome function, we show that the PLP-CaM interaction is important for organizing the PCM but is not essential for recruiting the proper amount of PCM. There are two possible explanations for this. First, it is possible that only a small amount of PLP (as seen with plp^{2KR}; plp^{-}) at the centriole is required to recruit, or load, PCM into the maturing centrosome, but a larger amount of PLP at the centriole (as seen with plp^{WT}; plp^{-} and plp^{2IQ}; plp^{-}) is required to stabilize the overall centrosome structure. In this case, the main role of the PLP-CaM interaction would be to efficiently recruit PLP to the centrosome, and the PLP-CaM interaction would not directly be involved in organizing the PCM. The second possible explanation is that CaM's interaction within the PACT domain is directly required for organizing Cnn. In this case, the main role of the PLP-CaM interaction would not be in recruiting PLP or Cnn, but instead it would be important to directly influence the organization of Cnn. Although our data do not directly support this second mechanism, it is worth noting that CDK5RAP2 (the Cnn human orthologue) interacts with CaM (Wang *et al.*, 2010) within a C-terminal region called Cnn motif 2 (CM2), which is conserved in *Drosophila* (Zhang and Megraw, 2007). One speculative model is that CaM is required to directly organize Cnn within the PCM by forming a tricomplex of Cnn-CaM-PLP, but this tricomplex would not be required for the initial recruitment of Cnn within the centriole vicinity. This model is worth exploring further through a dual structure–function study of PLP and Cnn. In addition, although this study focused on the role of the PLP-CaM interaction during mitosis, PLP has a recently reported negative regulatory role in PCM recruiting during interphase in *Drosophila* neuroblasts (Lerit and Rusan, 2013). If and how the PLP-CaM interaction plays a role during interphase and in the changes in the centrosome as it enters mitosis from interphase will be an interesting subject for future exploration.

A role for pericentrin has also been documented in ciliogenesis in human cultured cells and *Drosophila* mechanosensory neurons and sperm (Jurczyk *et al.*, 2004; Martinez-Campos *et al.*, 2004). In addition, CaM is a well-known axonemal component (Gitelman and Witman, 1980; Stommel *et al.*, 1982) and is important for ciliary function (AbouAlaiwi *et al.*, 2009; DiPetrillo and Smith, 2010; Plotnikova *et al.*, 2012). For these reasons, we investigated the importance of the PLP-CaM interaction for cilia function. Previous work showed that loss of PLP disrupts mechanosensation due to the loss of sensory organ mechanocilia, resulting in uncoordinated movements (Martinez-Campos *et al.*, 2004). The plp^{2KR}; plp^{-} flies also display an uncoordinated behavior indistinguishable from that of the null mutants, indicating that the PLP-CaM interaction is required for mechanosensation. We show that a likely cause of this defect is the inability of PLP^{2KR} to localize to neuronal centrioles and/or a loss of the localization of these centrioles to the base of the scolopale rods. It will be interesting to further investigate these centrioles to determine whether they have developed into neuronal basal bodies or whether they are fully formed basal bodies that are unable to

migrate and anchor to the cortex. The results of such experiments will help assign a more precise role for PLP in nucleating neuronal axonemes.

Finally, our analysis of the centriole-to–basal body transition during male spermatogenesis revealed the most surprising result of this study. We fully expected that the PLP-CaM interaction would be required for PLP function in building these basal bodies but were surprised to find that the *plp*^{2KR} allele fully rescues basal body formation, basal body integrity, and sperm motility. This suggests that the role of PLP in basal body formation might be cell type specific. This is not surprising, as basal body structure in each system is unique. The long basal bodies of the spermatid might only require low levels of PLP, whereas the smaller basal bodies of the sensory neurons might require high PLP levels. Another difference is that neuronal axoneme formation relies on intraflagellar transport (IFT), whereas formation of the sperm tail axoneme does not (Han *et al*., 2003; Sarpal *et al*., 2003). Consistent with a role in building IFT-dependent cilia, silencing pericentrin in RPE1 cells results in a reduction in the targeting of several IFT proteins to the basal body and a loss of primary cilia (Jurczyk *et al*., 2004). Therefore the PLP-CaM interaction might play a critical role in cilia/flagella built using IFT, and thus only the cilia in sensory neurons are affected.

In summary, we assigned critical roles for the PLP-CaM interaction in vivo, revealing a complicated, cell type–specific mechanism at work. Future work to identify other players, including the proteins that form the "docking site" for PACT, will be critical to begin to understand the interplay between pericentrin, CaM, Cnn, and these docking proteins. Posttranslational modifications, specific cell cycle control, protein isoforms, and cell type specificity are all critical elements to consider as the field moves toward understanding the details of centrosome proteins, including pericentrin.

MATERIALS AND METHODS

Fly stocks

All control (wild-type) flies used in this study are *yw*. The following strains were used: *plp*^{2172} (Spradling *et al*., 1999), *plp*^{5} (Martinez-Campos *et al*., 2004), Df(3L)BrdR15 (stock 5354; Bloomington *Drosophila* Stock Center, Bloomington, IN), actin-Gal4 (stock 3954; Bloomington *Drosophila* Stock Center), CaM-TRiP line (TRiP.HMS01318; stock 34609; Bloomington, IN), FRT^{42D},*cam*^{n339} (Heiman *et al*., 1996), and Ana1-tdTomato (Blachon *et al*., 2008). To generate the PLP wild-type (*plp*^{WT}) and mutant transgenes (*plp*^{2KR}, *plp*^{2IQ}), we first PCR amplified and directionally cloned full-length PLP^{PF} into pENTR/D vector for use in the Gateway cloning system. Site-directed mutagenesis was then conducted to generate *plp*^{2KR} and *plp*^{2IQ}. Each allele was recombined using Gateway reactions into the P-element destination vector pUWG (ubiquitin promoter, C-terminal GFP, DGRC). All transgenic flies were generated by BestGene (Chino Hills, CA) using standard P-element–mediated transformation.

Drosophila cell culture and double-stranded RNAi

Drosophila cell culture, in vitro dsRNA synthesis, and dsRNA treatments were performed as described previously (Rogers and Rogers, 2008). In brief, S2 and Kc cells were cultured in Sf900II medium (Life Technologies, Grand Island, NY) and split every 3–4 d. RNAi was performed in six-well tissue culture plates. Cells (50–90% confluency) were treated with 10 µg of dsRNA in 1 ml of medium and replenished with fresh medium/dsRNA every other day for 4–7 d. The following gene-specific primers were used to amplify DNA templates for RNA synthesis: control (5′-CGCTTTTCTGGATTCATCGAC-3′ and 5′-TGAGTAACCTGAGGCTATGG-3′), PLP (5′-TCAGTTTTTCCAGTGTTTTCTCC-3′ and 5′-TACAAACCAACGAAGAATTGGG-3′), CaM (5′-CGATCAGCTGACAGAGGA-3′ and 5′-AGTATTTCCCCCCACAATCC-3′), and Sas6 (5′-TTGAACACCGTACTCTTCTAC-3′ and 5′-CTTGAGGTCCTCGATTTTGT-3′).

Immunofluorescence

S2 and Kc cells were plated on #1.5 concanavalin A–coated coverslips and allowed to spread for 30–60 min. Cells were then briefly washed with phosphate-buffered saline (PBS) and fixed for 15 min in –20°C methanol. Cells were stained at room temperature in primary antibodies for 1 h and secondary antibodies for 30 min and mounted in Aqua-Poly/Mount (Polysciences, Warrington, PA). Whole brains dissected from third-instar larvae were fixed in 9% formaldehyde in PBSTx (PBS, 0.3% Triton X-100) for 15 min, washed 3× 15 min in PBSTx, and blocked for 1 h in PBT (PBS, 0.1% Tween-20, 1% bovine serum albumin [BSA]). For chordotonal neuron analysis, entire heads of third-day pupae were fixed as for brains for 20 min. Whole antennae were then removed from the heads. For testes imaging, larval or adult testes were dissected and fixed as for brains. Brains or testes were incubated in primary antibody in PBT plus 4% normal goat serum (NGS) overnight at 4°C. After several washes, samples were further blocked in modified PBT (PBS, 0.1% Tween-20, 2% BSA, and 4% NGS) and incubated for 2 h at room temperature with secondary antibody. Samples were finally washed 3× 15 min in PBST (PBS, 0.1% Tween-20) and mounted in Aqua-Poly/Mount. Primary antibodies used were rabbit anti-PLP (1:5000; Rogers *et al*., 2008), guinea pig anti-Asterless (1:30,000; gift from G. Rogers, University of Arizona Cancer Center, University of Arizona, Tucson, AZ), mouse anti-CaM (1:500, 05-173; Millipore), and rabbit anti-Cnn (1:2000, gift from T. Megraw (Florida State University, Tallahassee, FL; Heuer *et al*., 1995). Secondary antibodies were Alexa Fluor 488, 568, or 647 (1:500; Life Technologies). Phalloidin was used at 1:500 and added along with secondary antibodies for 3 h at room temperature with agitation.

Constructs and transfection

The synthesis of cDNA encoding full-length PLP^{PF} was commissioned from GenScript. This plasmid was used to template the PCR amplification of all PLP fragments (1–5) using the following primers: fragment 1 (5′-CACCATGAATCTGTACACTATATACGATTGG-3′ and 5′-AGGCGGATCCTGCTCCTCTTCC-3′), fragment 2 (5′-CACCATGTCCCTCTCCTTGGATGAGTC-3′ and 5′-TGGAGGTAGGGAGGAATGTG-3′), fragment 3 (5′-CACCATGGATCTTCAAGAGCATGCGGG-3′ and 5′-CAGCCGCTCGATTTCGCGC-3′), fragment 4 (5′-CACCATGACGCTGCAGGGTCGTATGGAGG-3′ and 5′-TTCATTGAAGTGTTCCAACTCTG-3′), fragment 5 (5′-CACCATGCGTTTAACCCTGCAAGCCAG-3′ and 5′-ATGATGCCGCGCATGCGCTC-3′). These fragments were directionally cloned into the pENTR/D vector for use in the Gateway cloning system (Life Technologies). Gateway recombination reactions were conducted using the manufacturer's protocols to tag each fragment with GFP or FLAG. For work in S2 cells, the pAWG (actin promoter, C-terminal GFP tag) destination vector was used, whereas the pAFW (actin promoter, N-terminal FLAG tag) destination vector was used to tag these same fragments with a 3xFLAG tag for the Co-IP experiments. Details on the pAWG and pAFW vectors can be found at the *Drosophila* Genomics Resource Center (DGRC; Bloomington, IN; https://dgrc.cgb.indiana.edu/Home) and the *Drosophila* Gateway website (http://emb.carnegiescience.edu/labs/murphy/Gateway%20vectors.html). To generate the GFP-40aaLinker-CaM construct, a CaM cDNA with a N-terminal 40 amino acid linker was PCR amplified from an unpublished vector provided by T. Megraw

and cloned into the pENTR/D vector. The 40aaLinker-CaM was then tagged using the Gateway system into pAGW (actin promoter, N-terminal GFP tag; DGRC) to generate GFP-40aaLinker-CaM. All deletions and point mutations were generated using the QuikChange II kit (Agilent Technologies) following the manufacturer's protocol. S2 or Kc Cells were transfected in a six-well plate containing a confluent monolayer of cells using Effectene (Qiagen, Venlo, Netherlands) by following the manufacturer's protocol. Cells were processed for immunofluorescence or immunoprecipitation 48 h posttransfection.

For mitochondrial targeting experiments, we modified the Gateway destination vector pAGW (actin promoter, N-terminal GFP tag; DGRC). We digested this vector with *Stu*I and *Age*I to remove the sequence for GFP and then ligated into its place a PCR product including the N-terminal 36 amino acids of the *Drosophila* Tom20 gene (gift of Hong Xu, National Heart, Lung, and Blood Institute, Bethesda, MD), followed immediately by the sequence encoding TagRFP. This new destination vector was named pAT20TRW. We then amplified the promoter, GFP, and calmodulin from the pAGW-40aaLinker-CaM construct described here and inserted it into the *Mlu*I site in the backbone of pAT20TRW, making pAT20TRW-AGFP-CaM. Fragments of PLP were then introduced into pAT20TRW-AGFP-CaM by standard Gateway cloning methods. These vectors allowed for simultaneous expression, from the same plasmid, of mitochondrial-targeted TagRFP-fusions of PLP fragments and GFP-calmodulin.

Immunoprecipitation and immunoblotting

S2 cells were cotransfected with GFP-CaM and each of the five FLAG-PLP fragments. Transfected cells were lysed in CLB (50 mM Tris, pH 7.2, 125 mM NaCl, 2 mM dithiothreitol, 0.1% Triton X-100, and 0.1 mM phenylmethanesulfonyl fluoride), precleared by centrifugation, and diluted to 5 mg/ml. Rabbit anti-GFP antibodies (clone ab290; Abcam, Cambridge, UK) were added to the lysate and rocked at 4°C for 60 min. Then 30 µl of equilibrated protein A Sepharose beads (Sigma-Aldrich, St. Louis, MO) were added to the lysates and rocked for an additional 60 min at 4°C. Beads were then washed three times in CLB and boiled for 5 min in SDS–PAGE sample buffer. The following primary antibodies were used for the Western blots in the Co-IP experiments: mouse anti-GFP (1:10,000, clone JL-8; Clontech Laboratories, Mountain View, CA) and mouse anti-FLAG (1:1000, clone M2; Sigma-Aldrich).

S2 cell extracts from dsRNA-treated cells (Supplemental Figure S1C) were produced by resuspending cell pellets in PBS plus 0.1%Triton X-100. SDS–PAGE sample buffer was added to the extracts and boiled for 5 min. Western blots were performed to determine knockdown efficiency. Tissue extracts from animals (Figure 4A) were generated by dissecting 20 brains from each genotype, adding them to 50 µl of 1× SDS–PAGE sample buffer, thoroughly grinding them using a microtubule pestle, and boiling the samples for 5 min. The following antibodies were used: mouse anti-calmodulin (1:500, MA3-917; Thermo Scientific), mouse anti–α-tubulin (1:5000, clone DM1a; Sigma-Aldrich), guinea pig anti-Sas6 (1:5000; gift from G. Rogers), and rabbit anti-PLP (1:5000; Rogers *et al.*, 2008).

Microscopy

All images were collected on a Nikon Ti Microscope equipped with a 100× (1.49 numerical aperture, polarization and total internal reflection fluorescence) objective, a CSU-22 spinning disk confocal head (Yokogawa, Tokyo, Japan), and an interline transfer-cooled charge-coupled device camera (CoolSNAP HQ2; Photometrics, Tuscon, AZ). Excitation laser was supplied by a laser merge module equipped with 491-, 561-, and 642-nm solid-state lasers (VisiTech International, Sunderland, UK). Emission filters (Semrock, Rochester, NY) were controlled by a MAC6000 (Ludl Electronic Products, Hawthorne, NY). The system is controlled with MetaMorph software (Molecular Devices, Sunnyvale, CA). For fixed cells, *Z*-stacks covering the entire volume of each cell were collected by acquiring optical slices spaced by 200 nm; these data are presented as maximum intensity projections.

Fluorescence measurements and statistical analysis

To determine the relative amount of wild-type and mutant PLP localization to centrioles in S2 cells (Figures 1 and 3 and Supplemental Figure S2), we used an empirical judgment of fluorescence intensity in a blind experiment to all genotypes. Cells were visualized on the microscope using epifluorescence to first identify the centriole marker by Asterless staining in the red channel. The filter cube was then switched to the green channel, where a judgment of fluorescence intensity was determined. This intensity was judged as strong, weak, or no signal. Figure 3 shows an example of a strong and no signal. A weak signal was assigned to anything between these two extremes. At least 200 cells per condition per trial were assayed in these experiments. Each independent trial was processed the same day and included both the wild-type (control dsRNA or full-length PLP) and non–wild-type (dsRNA treated or mutant *plp* alleles) cells. Three independent blind trials on three different days were conducted for each experiment shown in Figures 1 and 3 and Supplemental Figure S2; the average of all three trials is presented.

For fluorescence measurements in neuroblasts, cells of all measured genotypes were dissected and processed the same day. Measurements were always performed relative to the control for that specific day—this constituted a single experiment and was repeated in triplicate. Levels of Cnn and GFP were measured by adding the total intensity through the volume of the centrosome, which was then outlined with a region of interest (ROI) large enough to encompass the entire centrosome, and measurements of the total integrated intensity were collected. Background-integrated intensity was collected from an identical ROI in an adjacent cytoplasmic region and subtracted from the centrosome measurement to obtain a final value. For analysis of centrosome circularity (Figure 4), centrosome fluorescence was outlined by hand and analyzed using the shape descriptors in ImageJ (National Institutes of Health, Bethesda, MD). For measurement of cytoplasmic GFP levels, a region of cytoplasm of neuroblasts away from the centrosomes, nuclei, and all other notable cellular features was selected. The total fluorescence intensity of a 625-pixel^2 area of this region in a single confocal plane was measured, providing the total fluorescence of a fixed volume of cytoplasm. These data were normalized to the average total fluorescence intensity of PLP^{WT} (in WT). All images analyzed were digitized at 16 bit, and only a maximum of three-fourths of the full dynamic range of the camera was used to avoid saturation. ImageJ was used for all image analysis. All statistical analysis and plots were performed using Prism software (GraphPad, La Jolla, CA). All figures were assembled using PhotoDraw (Microsoft, Redmond, WA).

Yeast two-hybrid

Fragments of PLP and CAM were introduced into pDEST-pGADT7 and pDEST-pGBKT7 (Rossignol *et al.*, 2007) using the Gateway cloning system (Life Technologies). Before use in cloning, the kanamycin resistance cassette in pDEST-pGBKT7 was replaced with an ampicillin resistance cassette using yeast-mediated recombination. Fragments in pGADT7 or pGBKT7 were transformed into yeast strains Y187 and Y2HGold, respectively (Clontech, Mountain View, CA)

using standard techniques. Cultures of yeast carrying these plasmids were grown to OD_{600} ~0.5 at 30°C in SD Leu or SD –Trp media as appropriate to maintain plasmid selection. For mating, 20 µl of a Y187 strain and a Y2HGold strain were added to 100 µl of 2× yeast extract/peptone/dextrose medium in the well of a 96-well plate. Mating cultures were grown for 20–24 h at 30°C with shaking. Approximately 3 µl of cells were then pinned onto SD –Leu –Trp (DDO) plates using a Multi-Blot Replicator (VP 407AH; V&P Scientific), and plates were grown for 5 d at 30°C. These plates were replica plated onto four plates: 1) DDO, 2) QDO (SD –ade –leu -trp –ura), 3) DDOXA (SD –leu –trp plates containing Aureobasidin A (Clontech) and X-α-Gal (Gold Biotechnology, St. Louis, MO), 4) QDOXA (SD –ade –leu -trp –ura with Aureobasidin A and X-α-Gal). Plates were grown for 5 d at 30°C. Interactions were scored based on growth and development of blue color as appropriate. None of the plasmids used in this study was able to drive yeast-two hybrid reporter activity on its own (unpublished data).

CaM loss of function

We attempted to analyze the effect of CaM loss of function in vivo in two ways: first, we used actin-Gal4 to drive expression of uas-CaM RNAi using a TRiP line. No larvae were recovered from this cross at 25 and 29°C, precluding analysis of *cam*$^{-}$ cells in this manner. The second method was using the FRT flip system to create GFP-negative clones. Flies of the genotype hs-FLP;FRT^{42D},cam^{n339}/FRT42D, GFP^{nls} were heat shocked for 1, 2, or 3 h at 37°C, either 48 or 72 h after egg laying. Under no condition did we detect any GFP-negative cells. This suggests that cells are simply not viable without CaM, in agreement with data from budding yeast.

ACKNOWLEDGMENTS

We thank Jeremy Smyth for his comments and suggestions. N.M.R. is supported by the Division of Intramural Research at the National Heart, Lung, and Blood Institute/National Institutes of Health (1ZIAHL006126). G.C.R. is supported by National Cancer Institute/National Institutes of Health (P30CA23074) and GI SPORE (National Cancer Institute/National Institutes of Health, P50CA95060), the National Science Foundation (1158151), and the Arizona Biomedical Research Commission (1210). T.L.M. is supported by the National Institute of General Medical Sciences/National Institutes of Health (R01GM068756).

REFERENCES

AbouAlaiwi WA, Takahashi M, Mell BR, Jones TJ, Ratnam S, Kolb RJ, Nauli SM (2009). Ciliary polycystin-2 is a mechanosensitive calcium channel involved in nitric oxide signaling cascades. Circ Res 104, 860–869.

Anitha A, Nakamura K, Yamada K, Iwayama Y, Toyota T, Takei N, Iwata Y, Suzuki K, Sekine Y, Matsuzaki H, *et al*. (2008). Gene and expression analyses reveal enhanced expression of pericentrin 2 (PCNT2) in bipolar disorder. Biol Psychiatry 63, 678–685.

Basto R, Lau J, Vinogradova T, Gardiol A, Woods CG, Khodjakov A, Raff JW (2006). Flies without centrioles. Cell 125, 1375–1386.

Blachon S, Cai X, Roberts KA, Yang K, Polyanovsky A, Church A, Avidor-Reiss T (2009). A proximal centriole-like structure is present in *Drosophila* spermatids and can serve as a model to study centriole duplication. Genetics 182, 133–144.

Blachon S, Gopalakrishnan J, Omori Y, Polyanovsky A, Church A, Nicastro D, Malicki J, Avidor-Reiss T (2008). *Drosophila* Asterless and vertebrate Cep152 are orthologs essential for centriole duplication. Genetics 180, 2081–2094.

Choi YK, Liu P, Sze SK, Dai C, Qi RZ (2010). CDK5RAP2 stimulates microtubule nucleation by the gamma-tubulin ring complex. J Cell Biol 191, 1089–1095.

Delaval B, Doxsey SJ (2010). Pericentrin in cellular function and disease. J Cell Biol 188, 181–190.

Dictenberg JB, Zimmerman W, Sparks CA, Young A, Vidair C, Zheng Y, Carrington W, Fay FS, Doxsey SJ (1998). Pericentrin and gamma-tubulin form a protein complex and are organized into a novel lattice at the centrosome. J Cell Biol 141, 163–174.

DiPetrillo CG, Smith EF (2010). Pcdp1 is a central apparatus protein that binds Ca(2+)-calmodulin and regulates ciliary motility. J Cell Biol 189, 601–612.

Dobbelaere J, Josue F, Suijkerbuijk S, Baum B, Tapon N, Raff J (2008). A genome-wide RNAi screen to dissect centriole duplication and centrosome maturation in *Drosophila*. PLoS Biol 6, e224.

Doxsey SJ, Stein P, Evans L, Calarco PD, Kirschner M (1994). Pericentrin, a highly conserved centrosome protein involved in microtubule organization. Cell 76, 639–650.

Flory MR, Morphew M, Joseph JD, Means AR, Davis TN (2002). Pcp1p, an Spc110p-related calmodulin target at the centrosome of the fission yeast *Schizosaccharomyces pombe*. Cell Growth Differ 13, 47–58.

Flory MR, Moser MJ, Monnat RJ Jr, Davis TN (2000). Identification of a human centrosomal calmodulin-binding protein that shares homology with pericentrin. Proc Natl Acad Sci USA 97, 5919–5923.

Fong KW, Choi YK, Rattner JB, Qi RZ (2008). CDK5RAP2 is a pericentriolar protein that functions in centrosomal attachment of the gamma-tubulin ring complex. Mol Biol Cell 19, 115–125.

Fu J, Glover DM (2012). Structured illumination of the interface between centriole and peri-centriolar material. Open Biol 2, 120104.

Geiser JR, Sundberg HA, Chang BH, Muller EG, Davis TN (1993). The essential mitotic target of calmodulin is the 110-kilodalton component of the spindle pole body in *Saccharomyces cerevisiae*. Mol Cell Biol 13, 7913–7924.

Gillingham AK, Munro S (2000). The PACT domain, a conserved centrosomal targeting motif in the coiled-coil proteins AKAP450 and pericentrin. EMBO Rep 1, 524–529.

Gitelman SE, Witman GB (1980). Purification of calmodulin from *Chlamydomonas*: calmodulin occurs in cell bodies and flagella. J Cell Biol 87, 764–770.

Han YG, Kwok BH, Kernan MJ (2003). Intraflagellar transport is required in *Drosophila* to differentiate sensory cilia but not sperm. Curr Biol 13, 1679–1686.

Haren L, Stearns T, Luders J (2009). Plk1-dependent recruitment of gamma-tubulin complexes to mitotic centrosomes involves multiple PCM components. PLoS One 4, e5976.

Heiman RG, Atkinson RC, Andruss BF, Bolduc C, Kovalick GE, Beckingham K (1996). Spontaneous avoidance behavior in *Drosophila* null for calmodulin expression. Proc Natl Acad Sci USA 93, 2420–2425.

Heuer JG, Li K, Kaufman TC (1995). The *Drosophila* homeotic target gene centrosomin (cnn) encodes a novel centrosomal protein with leucine zippers and maps to a genomic region required for midgut morphogenesis. Development 121, 3861–3876.

Jackson AP, Griffith E, Walker S, Martin CA, Vagnarelli P, Stiff T, Vernay B, Al Sanna N, Saggar A, Hamel B, *et al*. (2008). Mutations in pericentrin cause Seckel syndrome with defective ATR-dependent DNA damage signaling. Nat Genet 40, 232–236.

Januschke J, Reina J, Llamazares S, Bertran T, Rossi F, Roig J, Gonzalez C (2013). Centrobin controls mother-daughter centriole asymmetry in *Drosophila* neuroblasts. Nat Cell Biol 15, 241–248.

Jurczyk A, Gromley A, Redick S, San Agustin J, Witman G, Pazour GJ, Peters DJ, Doxsey S (2004). Pericentrin forms a complex with intraflagellar transport proteins and polycystin-2 and is required for primary cilia assembly. J Cell Biol 166, 637–643.

Kantaputra P, Tanpaiboon P, Porntaveetus T, Ohazama A, Sharpe P, Rauch A, Hussadaloy A, Thiel CT (2011). The smallest teeth in the world are caused by mutations in the PCNT gene. Am J Med Genet A 155A, 1398–1403.

Kawaguchi S, Zheng Y (2004). Characterization of a *Drosophila* centrosome protein CP309 that shares homology with Kendrin and CG-NAP. Mol Biol Cell 15, 37–45.

Kellogg DR, Moritz M, Alberts BM (1994). The centrosome and cellular organization. Annu Rev Biochem 63, 639–674.

Kishi K, van Vugt MA, Okamoto K, Hayashi Y, Yaffe MB (2009). Functional dynamics of Polo-like kinase 1 at the centrosome. Mol Cell Biol 29, 3134–3150.

Lawo S, Hasegan M, Gupta GD, Pelletier L (2012). Subdiffraction imaging of centrosomes reveals higher-order organizational features of pericentriolar material. Nat Cell Biol 14, 1148–1158.

Lerit DA, Rusan NM (2013). PLP inhibits the activity of interphase centrosomes to ensure their proper segregation in stem cells. J Cell Biol 202, 1013–1022.

Martinez-Campos M, Basto R, Baker J, Kernan M, Raff JW (2004). The *Drosophila* pericentrin-like protein is essential for cilia/flagella function, but appears to be dispensable for mitosis. J Cell Biol 165, 673–683.

Matsumoto Y, Maller JL (2002). Calcium, calmodulin, and CaMKII requirement for initiation of centrosome duplication in *Xenopus* egg extracts. Science 295, 499–502.

Matsuo K, Nishimura T, Hayakawa A, Ono Y, Takahashi M (2010). Involvement of a centrosomal protein kendrin in the maintenance of centrosome cohesion by modulating Nek2A kinase activity. Biochem Biophys Res Commun 398, 217–223.

Megraw TL, Li K, Kao LR, Kaufman TC (1999). The centrosomin protein is required for centrosome assembly and function during cleavage in *Drosophila*. Development 126, 2829–2839.

Mennella V, Keszthelyi B, McDonald KL, Chhun B, Kan F, Rogers GC, Huang B, Agard DA (2012). Subdiffraction-resolution fluorescence microscopy reveals a domain of the centrosome critical for pericentriolar material organization. Nat Cell Biol 14, 1159–1168.

Muhlhans J, Brandstatter JH, Giessl A (2011). The centrosomal protein pericentrin identified at the basal body complex of the connecting cilium in mouse photoreceptors. PLoS One 6, e26496.

Plotnikova OV, Nikonova AS, Loskutov YV, Kozyulina PY, Pugacheva EN, Golemis EA (2012). Calmodulin activation of Aurora-A kinase (AURKA) is required during ciliary disassembly and in mitosis. Mol Biol Cell 23, 2658–2670.

Rauch A, Thiel CT, Schindler D, Wick U, Crow YJ, Ekici AB, van Essen AJ, Goecke TO, Al-Gazali L, Chrzanowska KH, *et al*. (2008). Mutations in the pericentrin (PCNT) gene cause primordial dwarfism. Science 319, 816–819.

Rebollo E, Sampaio P, Januschke J, Llamazares S, Varmark H, Gonzalez C (2007). Functionally unequal centrosomes drive spindle orientation in asymmetrically dividing *Drosophila* neural stem cells. Dev Cell 12, 467–474.

Rogers SL, Rogers GC (2008). Culture of *Drosophila* S2 cells and their use for RNAi-mediated loss-of-function studies and immunofluorescence microscopy. Nat Protoc 3, 606–611.

Rossignol P, Collier S, Bush M, Shaw P, Doonan JH (2007). Arabidopsis POT1A interacts with TERT-V(I8), an N-terminal splicing variant of telomerase. J Cell Sci 120, 3678–3687.

Rusan NM, Peifer M (2007). A role for a novel centrosome cycle in asymmetric cell division. J Cell Biol 177, 13–20.

Sarpal R, Todi SV, Sivan-Loukianova E, Shirolikar S, Subramanian N, Raff EC, Erickson JW, Ray K, Eberl DF (2003). *Drosophila* KAP interacts with the kinesin II motor subunit KLP64D to assemble chordotonal sensory cilia, but not sperm tails. Curr Biol 13, 1687–1696.

Sonnen KF, Schermelleh L, Leonhardt H, Nigg EA (2012). 3D-structured illumination microscopy provides novel insight into architecture of human centrosomes. Biol Open 1, 965–976.

Spradling AC, Stern D, Beaton A, Rhem EJ, Laverty T, Mozden N, Misra S, Rubin GM (1999). The Berkeley *Drosophila* Genome Project gene disruption project: single P-element insertions mutating 25% of vital *Drosophila* genes. Genetics 153, 135–177.

Stirling DA, Rayner TF, Prescott AR, Stark MJ (1996). Mutations which block the binding of calmodulin to Spc110p cause multiple mitotic defects. J Cell Sci 109, 1297–1310.

Stirling DA, Welch KA, Stark MJ (1994). Interaction with calmodulin is required for the function of Spc110p, an essential component of the yeast spindle pole body. EMBO J 13, 4329–4342.

Stommel EW, Stephens RE, Masure HR, Head JF (1982). Specific localization of scallop gill epithelial calmodulin in cilia. J Cell Biol 92, 622–628.

Sundberg HA, Goetsch L, Byers B, Davis TN (1996). Role of calmodulin and Spc110p interaction in the proper assembly of spindle pole body components. J Cell Biol 133, 111–124.

Takahashi M, Yamagiwa A, Nishimura T, Mukai H, Ono Y (2002). Centrosomal proteins CG-NAP and kendrin provide microtubule nucleation sites by anchoring gamma-tubulin ring complex. Mol Biol Cell 13, 3235–3245.

Varmark H, Llamazares S, Rebollo E, Lange B, Reina J, Schwarz H, Gonzalez C (2007). Asterless is a centriolar protein required for centrosome function and embryo development in *Drosophila*. Curr Biol 17, 1735–1745.

Wang Z, Wu T, Shi L, Zhang L, Zheng W, Qu JY, Niu R, Qi RZ (2010). Conserved motif of CDK5RAP2 mediates its localization to centrosomes and the Golgi complex. J Biol Chem 285, 22658–22665.

Willems M, Genevieve D, Borck G, Baumann C, Baujat G, Bieth E, Edery P, Farra C, Gerard M, Heron D, *et al*. (2010). Molecular analysis of pericentrin gene (PCNT) in a series of 24 Seckel/microcephalic osteodysplastic primordial dwarfism type II (MOPD II) families. J Med Genet 47, 797–802.

Yap KL, Kim J, Truong K, Sherman M, Yuan T, Ikura M (2000). Calmodulin target database. J Struct Funct Genomics 1, 8–14.

Zavortink M, Welsh MJ, McIntosh JR (1983). The distribution of calmodulin in living mitotic cells. Exp Cell Res 149, 375–385.

Zhang J, Megraw TL (2007). Proper recruitment of gamma-tubulin and D-TACC/Msps to embryonic *Drosophila* centrosomes requires centrosomin motif 1. Mol Biol Cell 18, 4037–4049.

Zimmerman WC, Sillibourne J, Rosa J, Doxsey SJ (2004). Mitosis-specific anchoring of gamma tubulin complexes by pericentrin controls spindle organization and mitotic entry. Mol Biol Cell 15, 3642–3657.